EMBO reports

TRANSPARENT PROCESS

scientific report

SpoIIIE mechanism of directional translocation involves target search coupled to sequence-dependent motor stimulation

Diego I. Cattoni[1], Osvaldo Chara[2,3], Cédric Godefroy[1], Emmanuel Margeat[1], Sonia Trigueros[4], Pierre-Emmanuel Milhiet[1] & Marcelo Nöllmann[1+]

[1]Centre de Biochimie Structurale, CNRS UMR5048, INSERM U1054, Université de Montpellier I & II, Montpellier, France, [2]Institute of Physics of Liquids and Biological Systems (CONICET, UNLP), La Plata, Argentina, [3]Center of High Performance Computing, Technische Universität Dresden, Dresden, Germany, and [4]Department of Physics, University of Oxford, Oxford, UK

SpoIIIE/FtsK are membrane-anchored, ATP-fuelled, directional motors responsible for chromosomal segregation in bacteria. Directionality in these motors is governed by interactions between specialized sequence-recognition modules (SpoIIIE-γ/FtsK-γ) and highly skewed chromosomal sequences (SRS/KOPS). Using a new combination of ensemble and single-molecule methods, we dissect the series of steps required for SRS localization and motor activation. First, we demonstrate that SpoIIIE/DNA association kinetics are sequence independent, with binding specificity being uniquely determined by dissociation. Next, we show by single-molecule and modelling methods that hexameric SpoIIIE binds DNA non-specifically and finds SRS by an ATP-independent target search mechanism, with ensuing oligomerization and binding of SpoIIIE-γ to SRS triggering motor stimulation. Finally, we propose a new model that provides an entirely new interpretation of previous observations for the origin of SRS/KOPS-directed translocation by SpoIIIE/FtsK.

Keywords: translocation directionality; sequence-specific regulation; DNA segregation; molecular motors; single molecule

EMBO *reports* advance online publication 5 April 2013; doi:10.1038/embor.2013.39

INTRODUCTION

Several key bacterial cellular processes, including chromosome segregation, viral DNA packaging and intercellular gene transfer require the transport of double-stranded DNA (dsDNA) within and between cellular compartments. SpoIIIE/FtsK/TraB are ring-shaped, membrane-anchored, ATP-fuelled, directional motors required to segregate DNA across membranes during sporulation, cell division and conjugation [1–3]. *Bacillus subtilis* SpoIIIE and *Escherichia coli* FtsK are highly homologous proteins composed of an N-terminal trans-membrane domain, a putatively unstructured linker and a highly homologous C-terminal motor domain involved in dsDNA translocation. The SpoIIIE/FtsK motor assembles as a hexameric ring that binds dsDNA through its central channel, and is composed of three separate subdomains: α, β and γ, with α and β being responsible for DNA translocation and ATP hydrolysis. Translocation directionality in these motors is regulated by orientation-specific interactions between γ-domains and highly skewed octameric chromosomal DNA sequences called SRS for SpoIIIE (SpoIIIE recognition sequence, Ptacin *et al* [2]) and KOPS for FtsK (FtsK-orienting polar sequences [4,5]). γ-domains fold as winged-helix motifs and bind as trimers to single KOPS [6].

The most prominent model to explain the molecular mechanism by which SRS/KOPS direct SpoIIIE/FtsK movement (preferential loading model) is depicted in Fig 1A [7]. In this model, translocation directionality is established by an orientation-specific assembly of SpoIIIE/FtsK monomers onto SRS/KOPS, which unambiguously define the initial translocation direction of the motor [6,8]. Here, we use a combination of ensemble, single-molecule and modelling methods to quantitatively investigate the mechanism by which SpoIIIE finds SRS.

RESULTS

The preferential loading model proposes that SpoIIIE/FtsK assemble at SRS/KOPS in an orientation-specific manner to confer directional translocation. To test this hypothesis, we performed anisotropy-based measurements of pre-equilibrium and equilibrium binding of SpoIIIE to DNA fragments containing two SRS sequences in tandem repeat or a non-specific DNA sequence (G-rich as SRS but not recognized by SpoIIIE [2]) (hereafter,

[1]Centre de Biochimie Structurale, CNRS UMR5048, INSERM U1054, Université de Montpellier I & II, 34090 Montpellier, France
[2]Institute of Physics of Liquids and Biological Systems (CONICET, UNLP), 1900 La Plata, Argentina
[3]Center of High Performance Computing, Technische Universität Dresden, 01062 Dresden, Germany
[4]Department of Physics, University of Oxford, Oxford OX1 3PU, UK
[+]Corresponding author. Tel: +33 04 67 41 79 12; Fax: +33 04 67 41 79 13; E-mail: marcelo.nollmann@cbs.cnrs.fr

Received 4 January 2013; revised 5 March 2013; accepted 11 March 2013; published online 5 April 2013

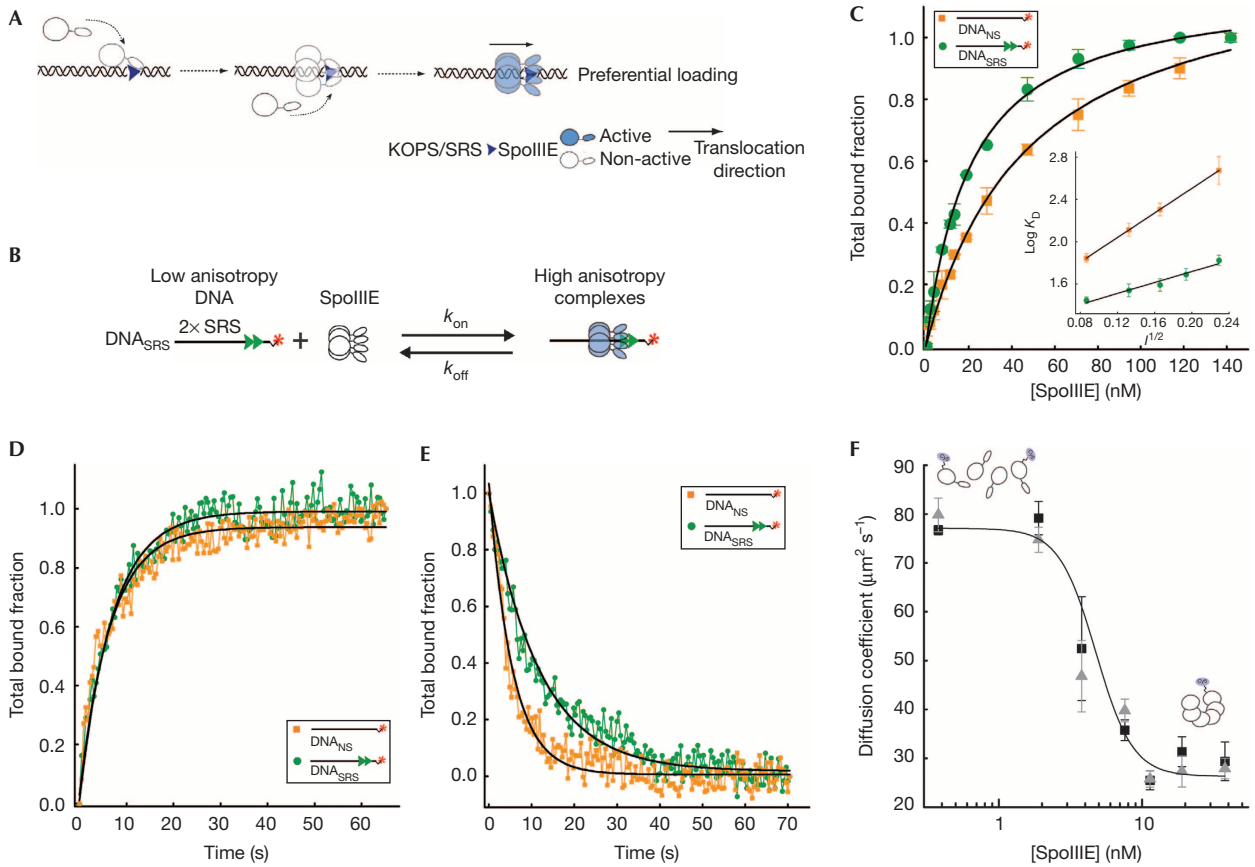

Fig 1 | Pre-formed SpoIIIE hexamers bind specifically but do not load onto SRS. (**A**) Scheme representing the preferential loading model proposed for FtsK/SpoIIIE sequence recognition and translocation mechanism. (**B**) Scheme representing the experimental set-up for fluorescence anisotropy measurements of SpoIIIE–DNA-binding equilibrium and kinetics. (**C**) SpoIIIE-binding isotherms for DNA_{SRS} and DNA_{NS}. Solid line represents the fitting of equation S2 (supplementary information online) to experimental data (see best fitting parameters in main text). Inset shows affinity changes of SpoIIIE for DNA_{SRS} and DNA_{NS} versus ionic strength (I) of monovalent salt (NaCl). (**D**) On-rate kinetics of SpoIIIE binding to DNA_{SRS} and DNA_{NS}. (**E**) Off-rate kinetics of SpoIIIE dissociation from DNA_{SRS} and DNA_{NS}. Solid lines in **D** and **E** represent the fit of equation S3 and S4 (supplementary information online) to experimental data (see main text for best fitting parameters). (**F**) Diffusion coefficients of Cy5-labelled SpoIIIE versus protein concentration in presence (grey triangles) or absence (black squares) of DNA_{SRS} obtained from FCS measurements. Solid line represents the fitting of model M1 to the experimental data (see main text for fitting parameters). In panels **C** and **F**, error bars represent s.d. with $n = 5$ and 3, respectively.

DNA_{SRS} and DNA_{NS}). The binding of large proteins, such as SpoIIIE, to short fluorescently labelled DNA fragments decreases the rotational diffusion of the DNA molecule and increases the fluorescence anisotropy of the attached fluorophore (Fig 1B) [9]. This signal is used to determine the total bound fraction as a function of protein concentration (supplementary information online). The binding isotherms were well fitted by a single-site-binding model; leading to a K_D of 22 ± 4 nM for DNA_{SRS} and 61 ± 12 nM for DNA_{NS} (Fig 1C; supplementary Fig S1A online and supplementary information online). The affinity of SpoIIIE to DNA_{SRS} remained only 2–3 times higher than that of DNA_{NS} even at high ionic strength conditions (inset Fig 1C; supplementary Fig S1B), thus electrostatic interactions influence the binding affinity of SpoIIIE but not its specificity.

Next, we measured the kinetics of binding of SpoIIIE to SRS and non-specific DNA sequences. The association and dissociation (triggered by addition of an excess of non-labelled DNA_{NS} as competitor) binding kinetics showed a single exponential behaviour (Fig 1D,E; supplementary information online) suggesting that association and dissociation occur through a monomolecular process not disturbed by additional dispersive factors such as oligomerization on binding to DNA (see below). The apparent association rates (k_{on}^{app}) were obtained from the decay constant of single exponential fits to the association curves. The apparent association rates were $0.23 \pm 0.04\,s^{-1}$ for DNA_{NS} and $0.21 \pm 0.03\,s^{-1}$ for DNA_{SRS}, demonstrating that the presence of SRS does not affect the kinetics of SpoIIIE association to DNA (Fig 1D). In contrast, the dissociation rate constant (k_{off}) of SpoIIIE from DNA_{NS} was $0.14 \pm 0.02\,s^{-1}$, whereas that from DNA_{SRS} was 2.3 times slower ($0.06 \pm 0.01\,s^{-1}$) (Fig 1E; supplementary Table S1 online). Assuming that the rate constants are unimolecular, from the K_D and k_{off} values obtained for each substrate, we can estimate a second-order association rate constant (k_{on}) of $(2.2 \pm 0.7) \times 10^6\,M^{-1}s^{-1}$ for DNA_{NS} and $(2.6 \pm 0.9) \times 10^6\,M^{-1}s^{-1}$ for DNA_{SRS} (see discussion in supplementary Fig S1 online). Similar results were obtained when second-order association rate constants were

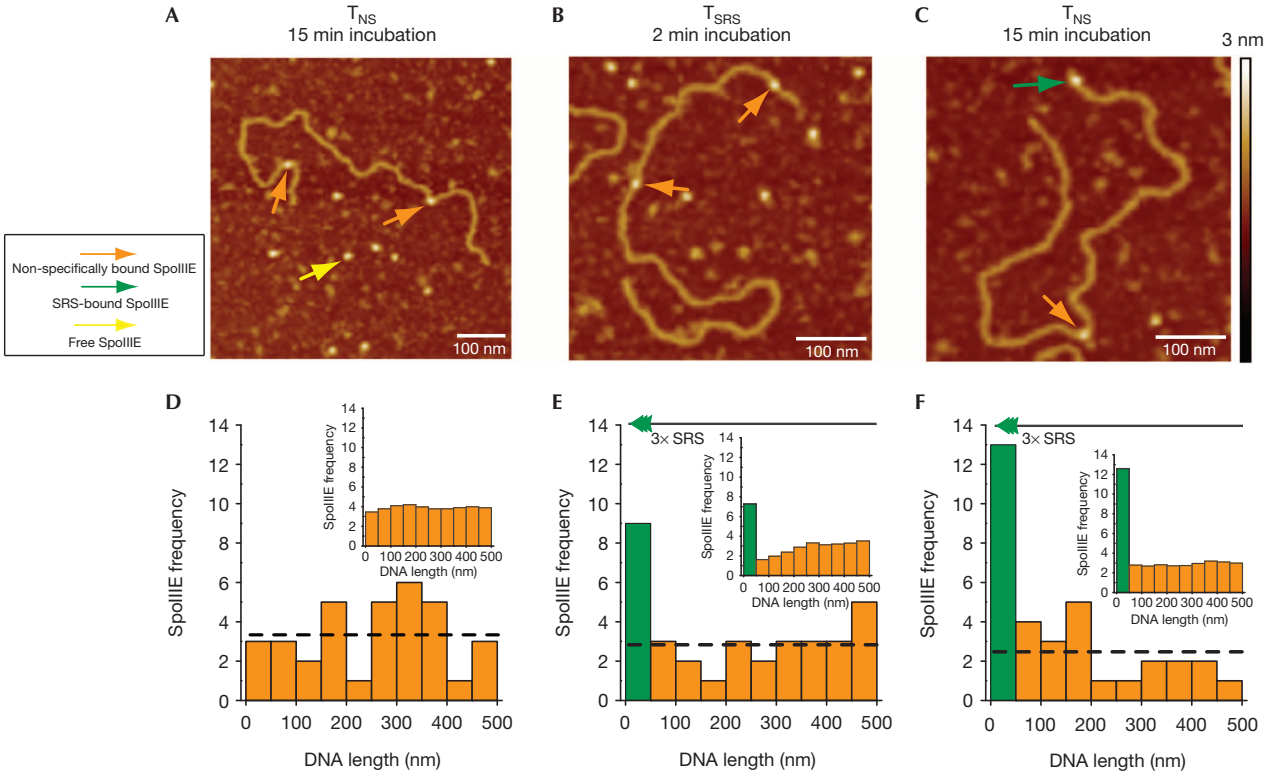

Fig 2 | Hexameric SpoIIIE binds to non-specific DNA and finds SRS by an ATP-independent mechanism. (**A–C**) AFM imaging of SpoIIIE–DNA complexes. Yellow arrow indicates free SpoIIIE, orange arrows indicate SpoIIIE bound to non-specific DNA sequences and green arrows indicate SpoIIIE–SRS complexes. (**A**) T_{NS} substrates incubated with SpoIIIE for 15 min. (**B–C**) T_{SRS} substrates incubated with SpoIIIE for 2 and 15 min, respectively. (**D–F**) Histograms of SpoIIIE distributions on DNA for the different substrates and incubation times described in **A–C**. SpoIIIE position in DNA was measured as the minimum distance of SpoIIIE particles to the end of DNA. A total of 35–40 individual SpoIIIE–DNA complexes were analysed for each condition. Dashed line indicates the average frequency of SpoIIIE complexes expected for an ideally homogenous distribution in T_{NS} substrates. Insets in **D–F** show the simulated SpoIIIE distributions in different DNA substrates obtained from Monte Carlo modelling using model II. Detailed description and simulations parameters are given in supplementary information online and supplementary Table S2 online.

estimated from the k_{on}^{app} and k_{off} values using equation S5 in supplementary information online and supplementary Table S1 online. These results indicate that the difference observed in the K_D measurements for DNA_{NS} and DNA_{SRS} ($\sim$2.7) rises from the effect of a slower dissociation of SpoIIIE from DNA_{SRS}, rather than an increase in association rate in the presence of SRS. The equilibrium and binding kinetics of SpoIIIE were not significantly affected in the presence of ATP or ADP and no significant changes in the K_D and k_{on}/k_{off} ratio were observed (supplementary Table S1 online). These results indicate that SRS sequences slow down the dissociation of SpoIIIE from DNA rather than speeding up its association to SRS-containing DNA.

Our binding results indicate that SpoIIIE binds to DNA in a single step with no cooperativity, however previous studies proposed that SRS/KOPS sequences serve as a nucleation platform for the hexamerization of FtsK [8]. To further test the SpoIIIE–DNA complex assembly mechanism, we monitored the oligomeric state of SpoIIIE on the basis of its diffusional properties. On the basis of computational methods [10], we estimate that monomeric SpoIIIE has a diffusion coefficient of 69 $\mu m^2 s^{-1}$, whereas that of hexameric SpoIIIE is 36 $\mu m^2 s^{-1}$. We experimentally determined the solution diffusion coefficient of fluorescently labelled SpoIIIE as a function of protein concentration in the absence or presence of DNA by fluorescence correlation spectroscopy (FCS) (Fig 1F; supplementary Fig S2B,C online). Diffusion coefficients measured by FCS were in good agreement with the values predicted by modelling, indicating that SpoIIIE exists in a monomeric form at low concentrations (<1 nM monomer) and predominantly in hexameric form at high concentrations (>6 nM monomer). Assuming a simple equilibrium between monomeric and hexameric species (supplementary information online) we determined an oligomerization dissociation constant of 5 ± 2 nM. Interestingly, these results did not depend on the presence of DNA (Fig 1F; supplementary Fig S2C,D online and supplementary Table S2 online), and suggest that SpoIIIE binds DNA as a pre-formed hexameric ring. On the basis of our binding experiments, we can estimate that the affinity of hexameric SpoIIIE is 2.1 ± 0.4 nM for DNA_{SRS} and 6 ± 1 nM for DNA_{NS}.

These results indicate that SpoIIIE neither loads nor assembles at SRS, but how else is SpoIIIE translocation directionality established? To address this question, we evaluated the distribution of SpoIIIE in long DNA substrates containing or not SRS sequences by atomic force microscopy (AFM). Two DNA substrates were designed (T_{NS} and T_{SRS}) consisting of a 3-kbp antenna region devoid of SRS sequences, and a tandem repeat of either SRS or non-specific DNA (same sequence used in DNA_{NS},

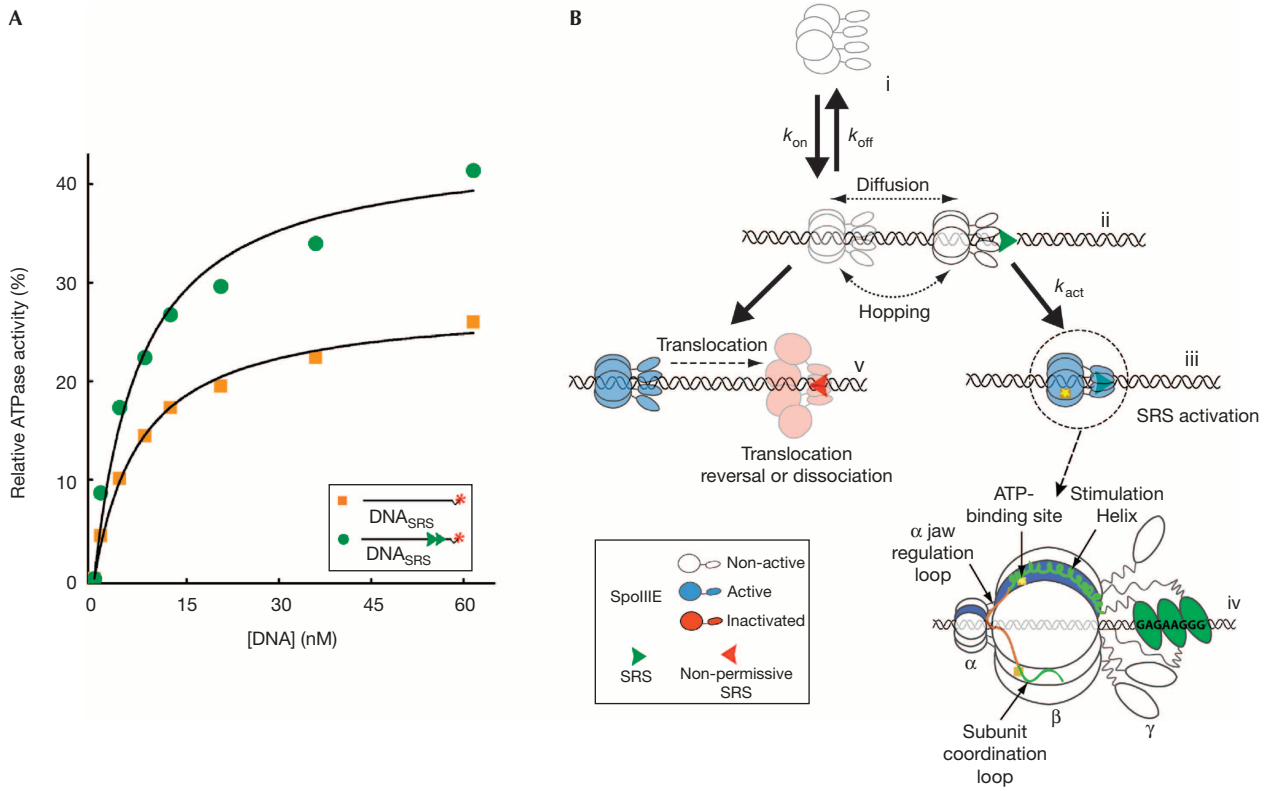

Fig 3 | Proposed mechanism for sequence-directed SpoIIIE directional translocation. (**A**) Relative ATPase activity as a function of DNA concentration. Solid line represents fit of equation S9 (supplementary information online) to data with $V_{max} = 2.6 \pm 0.1$ for DNA_{NS} and 4.1 ± 0.3 for DNA_{SRS}. Relative ATPase activities are obtained by normalizing the ATPase activity of SpoIIIE on DNA_{SRS} or DNA_{NS} by the ATPase activity in saturating amounts of λ-DNA ($\approx$10 mol ATP per second per mol SpoIIIE). (**B**) Schematic representation of the target search and sequence-specific activation model (see main text). (**B**-iv) Schematic representation of a SpoIIIE hexamer binding SRS and structural elements proposed to be involved in sequence-specific activation of the motor (see supplementary Fig S6 online for high-resolution model). Stimulation helix is shown in green, subunit coordination loop in dark green and α jaw regulation loop in brown. (**B**-v) Actively translocating SpoIIIE can interact with non-permissive SRS sequences leading to SpoIIIE dissociation [2] or translocation reversal [1,7].

see supplementary Fig S3D online) 70 bp away from the DNA end. SpoIIIE was incubated with T_{NS} or T_{SRS} (at 2:1 hexamer:DNA ratio, [DNA] = 1 nM) without ATP for either 2 or 15 min before deposition onto a mica surface. Images of free and DNA-bound SpoIIIE are shown in Fig 2. Consistently with our FCS measurements and electron microscopy images (unpublished observations), the size of free and DNA-bound SpoIIIE particles (full width at half maximum of 12 ± 0.5 nm) is compatible with the hexameric crystal structure of FtsK (hexamer size ~12 nm) [11], independently of the presence or not of SRS (Fig 2A; supplementary Fig S3A–C online). These observations rule out models in which the unit of translocation is a head-to-head dodecamer [1,11] and is in contradiction with the model of Graham *et al* [8] in which FtsK hexamer assembly is KOPS dependent. An automated algorithm was used to trace the DNA contour and to determine the precise localization of SpoIIIE hexamers with respect to DNA ends (supplementary information online). The distribution of SpoIIIE on T_{NS} is homogeneous, independently of incubation time (Fig 2D; supplementary Fig S3D). In contrast, at short incubation times with T_{SRS}, there is a ~2.5-fold excess of SpoIIIE hexamers at the position of SRS sequences with respect to proteins localized elsewhere (Fig 2E). Notably, this migration of SpoIIIE from non-specific DNA sequences to SRS increases over time until reaching a ~4-fold excess after 15 min of incubation (Fig 2F). Similar experiments in which SRS was located on the middle of a linear DNA fragment show a redistribution of SpoIIIE to this site, demonstrating that the bias in SpoIIIE localization is not due to a preference of SpoIIIE to bind DNA ends (supplementary Fig S3E online).

Taken together, our binding, FCS and AFM results indicate that SpoIIIE does not assemble preferentially on SRS. It is well established that proteins that interact with specific DNA sequences are typically able to reach their target sequence by a mechanism that involves one-dimensional (1D) diffusion ('sliding') or/and 3D 'hopping' [12]. To test these possible mechanisms for SpoIIIE, we used Monte Carlo simulations. We modelled three different mechanisms by which SpoIIIE can reach SRS (supplementary Fig S4 online): (1) repetitive cycles of DNA binding and dissociation (model I), (2) binding/dissociation to/from DNA and sliding (model II) and (3) binding/dissociation to/from DNA and intramolecular hopping (model III). For each model, we predicted the distributions of localizations observed by AFM with association and dissociation constants to non-specific and SRS sequences fixed to values obtained from our binding experiments

(discussed in supplementary Fig S4 online). We observed that model I did not fit the AFM distributions for T_{SRS} under any set of parameters (supplementary Fig S4B online). In contrast, when using model II or III, at equilibrium, SpoIIIE preferentially located to SRS sites in T_{SRS} and homogeneously in T_{NS}, as observed experimentally (insets in Fig 2D,F; supplementary Fig S4C,D online). These distributions were obtained with sliding lengths of 90 ± 22 bp and 1 ± 0.25 bp for non-specific and SRS DNA, and with hopping probabilities of 0.7 and 0.006 for non-specific and SRS sequences (supplementary Table S3 online). As expected, at shorter times, the preferential localization of SpoIIIE to SRS in T_{SRS} was less marked and showed asymmetries similar to those observed after a 2-min incubation (inset in Fig 2E; supplementary Fig S4C,D online). For both models II and III, we observed that stable SpoIIIE localization to SRS required an asymmetry in sliding lengths or hopping probabilities between SRS and non-specific sites ($sld^{NS}/sld^{SRS} = 90$, $p_{hopp}{}^{NS}/p_{hopp}{}^{SRS} = 116$, see supplementary Fig S4D online for further discussion), indicating that preferential dissociation from non-specific sites rather than from SRS is not the only mechanism responsible for anchoring SpoIIIE to SRS.

Overall, these data indicate that SpoIIIE specifically localizes to SRS by a mechanism that involves binding to a non-specific DNA and target search exploration by either or both sliding or/and hopping, but do not indicate the ensuing steps following specific SRS recognition. A possible mechanism that could lead to directional motion involves orientation-specific activation of SpoIIIE by SRS. To test this hypothesis, we measured the ATPase activity of SpoIIIE in the presence of increasing concentrations of DNA_{SRS} or DNA_{NS}. ATP hydrolysis rates increased as a function of DNA concentration for both substrates (Fig 3A; supplementary Fig S5 online). From the fitting of a quadratic function (supplementary information online) to the data, the maximal activity of SpoIIIE at saturating concentrations of DNA_{SRS} (V_{max}) was $\sim$1.6-fold higher than for DNA_{NS} (Fig 3A), suggesting a stimulation of the motor on SRS binding by SpoIIIE-γ (see discussion in supplementary Fig S5 online). To further test this model, we performed binding affinity and ATPase measurements of SpoIIIE-γ mutants (supplementary Fig S5E,F online). These studies show a relevant role of SpoIIIE-γ in the regulation of ATPase activity, and suggest that both specific SpoIIIE-γ/SRS interactions and oligomerization of SpoIIIE-γ are required for the stimulation of the activity of the motor domain (see supplementary Fig S5 online for further discussion).

DISCUSSION

During sporulation and cell division, directional chromosomal segregation by SpoIIIE and FtsK involves specific interactions between SpoIIIE-γ/Ftsk-γ and SRS/KOPS. Recently, it was proposed that the mechanism by which FtsK-γ/KOPS interactions lead to motor directionality involves orientation-specific assembly of active FtsK hexamers on DNA specifically at KOPS [6,8]. In this paper, we propose a conceptually different, alternative model for directionality of SpoIIIE/FtsK motors that involves three sequential steps (Fig 3B): (i) binding of pre-formed hexamers to non-specific DNA, (ii) specific localization of SpoIIIE to SRS by target search exploration involving either or both sliding and/or hopping and (iii) sequence-specific activation of the motor mediated by binding and oligomerization of SpoIIIE-γ on SRS. As previously proposed, other mechanisms involving orientation-specific SpoIIIE-γ/SRS interactions could account for the maintenance of directional movement of actively translocating motors (Fig 3B-v) [1,2,7].

Several independent lines of evidence demonstrate that SpoIIIE does not assemble on DNA but rather binds DNA as a pre-formed hexamer. First, our solution FCS experiments clearly show that the hexamerization constant of SpoIIIE (5 nM) is four times lower than the K_D for SpoIIIE/SRS binding (22 nM). Second, AFM imaging shows that SpoIIIE is hexameric in the presence or absence of DNA at concentrations below the K_D for SRS binding. Third, all binding data could be fitted with a single-species kinetic model, ruling out cooperative SpoIIIE assembly on DNA. Finally, $\sim$70 monomers of SpoIIIE localize on sporulating septa *in vivo* [13], translating into a local *in vivo* concentration of $\sim$1 μM; a concentration at which SpoIIIE should be fully hexamerized before DNA binding. Our results are not consistent with the KOPS-mediated hexamerization mechanism proposed for FtsK [8], as we show that SRS sequences do not have a role in protein assembly. In fact, in that and other studies [6,7], incubation of FtsK with DNA could have led to non-specific DNA binding with ensuing localization to KOPS by sliding/hopping, as proposed in our model. We consider that the binding of pre-formed hexamers to dsDNA might involve conformational transitions from an open- (inactive) to a closed-ring structure (active), as previously shown for other hexameric nucleic-acid motors [14]. These structural transitions might be favored by orientation-specific SpoIIIE–SRS interactions (see below), a mechanism that would provide directionally-biased motor activation.

Second, our kinetic studies showed that SpoIIIE association rates are sequence-independent, and do not depend on ionic conditions or nucleotide-bound state. In addition, AFM imaging proved that hexameric SpoIIIE efficiently binds non-specific DNA at extremely low concentrations ($\sim$2 nM hexamer). Importantly, SRS/KOPS sequences are very sparsely distributed in the *B. subtilis* and *E. coli* chromosomes (in average, one SRS/15 kb, one KOPS/3.5 kb). Taken together, these results indicate that the first step towards the establishment of directional translocation involves association of pre-formed SpoIIIE hexamers to non-specific DNA. In contrast, the preferential loading model posits that the pathway through which FtsK finds KOPS involves 3D diffusion from solution without interaction with other DNA sequences [6–8,15]. This model is counterintuitive as protein–DNA association rates are rather dominated by molecular mass, size and charge [12], and not by interaction specificity. Indeed, specific contacts between SpoIIIE-γ and SRS (that are not present when SpoIIIE interacts with DNA_{NS}) should lead to an increase in interaction free energy and thereby to a decrease in the dissociation rate, as we observed experimentally.

Our equilibrium-binding studies revealed that SpoIIIE binds SRS with a relatively low specificity (2.5-fold increase in affinity with respect to DNA_{NS}) that is independent of ionic strength or nucleotide-bound state. This, coupled to the scarce frequency of chromosomal SRS sequences, raises the question of how can SRS be efficient at directing SpoIIIE movement. AFM imaging showed that SpoIIIE motors initially bind DNA non-specifically but can efficiently scan a long DNA substrate (3 kb) to locate and remain stably bound to SRS. Monte Carlo modelling further showed that this process could be explained by a target search mechanism, involving either or both sliding or/and hopping, two common mechanisms for DNA-binding proteins to find their specific

binding sites [12]. In addition, these simulations proved that the main mechanism maintaining SpoIIIE stably bound to sparsely distributed SRS involves a slow, asymmetric rate of sliding/hopping out of SRS. Thus, despite the low SRS specificity and the sparse chromosomal distribution of SRS, SpoIIIE can rapidly and efficiently find and localize to SRS before ATP-fuelled translocation is fully engaged. Even with a relatively short linker domain (~30 nm if extended), septum-tethered SpoIIIE can explore a large chromosomal region (~200 kbp) due to the high degree of DNA compaction in the axial filament during septal invagination.

Previously, ATPase stimulation by KOPS was interpreted as evidence that FtsK loads on KOPS [7]. Instead, our data showed that the maximal ATPase activity of the SpoIIIE motor is stimulated by SRS, and suggested that this process not only requires specific SpoIIIE-γ/SRS binding but also SpoIIIE-γ oligomerization. Intriguingly, ATP hydrolysis occurs close to the SpoIIIE-αβ interphase, and considerably far (~45 Å) from the location of SpoIIIE-γ/SRS complexes (Fig 3B-iv; supplementary Fig S6 online). But then, how is SRS-recognition information channelled across the β-subdomain into the ATP hydrolysis and DNA translocation domains of the motor? Surprisingly, the mechanism involved in this communication could be relatively simple. SpoIIIE-αβ form the hexameric motor domain, with SpoIIIE-α being responsible for DNA translocation [11] and ATP hydrolysis taking place at the interface between neighbouring SpoIIIE-β monomers (Fig 3B-iv; supplementary Fig S6 online). SpoIIIE-γ is attached to the opposite end of SpoIIIE-β by an unconserved and unstructured linker, which connects SpoIIIE-γ directly to the site of ATP hydrolysis through a loop and an external helix, both of which are highly conserved (stimulation helix, Fig 3B-iv; supplementary Fig S6 online). Interestingly, the stimulation helix is directly connected to a loop involved in the formation of the ATP-binding pocket and hardwired to the ATP-binding site at the neighbouring subunit in a counter-clockwise manner (subunit coordination loop, Fig 3B-iv; supplementary Fig S6 online). Thus, oligomerization and binding of SpoIIIE-γ to SRS could lead to rotations or translations of the stimulation helix that would directly affect ATP-binding pocket accessibility, DNA translocation and inter-subunit coordination. In fact, recent evidence suggests that the sliding of well-anchored external helices can serve as a mechanism for long-range communication between different protein domains and affect the catalytic activity of an enzyme [16]. This mechanism of communication between sequence recognition and motor domains could favour the conversion of SpoIIIE from pre-formed to active hexamers at SRS, as well as regulate motor activity after orientation-specific recognition of SRS by actively translocating motors.

Overall, our new mechanism involving diffusional target search coupled to sequence-specific motor activation provides an alternative and conceptually distinct explanation to previous observations [6–8] and does not require preferential assembly onto SRS/KOPS sequences as previously believed. This mechanism might be applicable to other dsDNA translocases involved in bacterial conjugation (TraB) or chromosome dimer resolution (Sfta), might be relevant to other motors with similar domain architecture, such as the transcription termination factor Rho [14] or bacterial replication initiation factors (DnaA [17]) and represents a new regulatory mechanism for the activity of ring-shaped motors in general.

METHODS

SpoIIIE purification, labelling and activity. SpoIIIE and mutants were expressed and purified as described [2]. The N-terminal end of the SpoIIIE motor was covalently labelled with Cy5 mono NHS-ester dye (Amersham Biosciences), excess dye was removed by affinity purification. This modification did not affect the ATPase activity of SpoIIIE (supplementary Fig S2A online). More details are provided in supplementary information online.

Fluorescence anisotropy and ATPase activity. Fluorescence anisotropy (FA) experiments used short, 5′-Cy3-labelled DNA fragments (43 bp, DNA_{NS} and DNA_{SRS}, Eurogentec), with the following sequences: DNA_{SRS}: 5′-GC**GAGAAGGGAGAAGGG**AGATCTTACCGCTGTTGAGATCCAGC-3′. DNA_{NS}: 5′-GCGGAGGCGGGAGGCGGAGATCTTACCGCTGTTGAGATCCAGC-3′ where bold characters highlight the bases containing two overlapping SRS sequences. For equilibrium binding, FA measurements were performed at 27 °C using a microplate reader (TECAN Safire2). Measurements were performed in 50 mM Tris (pH 7.5), 0.15 mg ml^{-1} of BSA, 3% glycerol, 7.5 mM NaCl and 10 mM $MgCl_2$ (hereafter, reaction buffer). Pre-equilibrium binding experiments were performed at 27 °C using a rapid mixing device coupled to an ISS K2 spectrofluorometer (ISS, Champaign, Illinois). Association experiments were started by mixing equal volumes of 100 nM SpoIIIE with 2 nM DNA (DNA_{NS} or DNA_{SRS}) and FA signal was followed over time. In dissociation experiments, a mixture of 100 nM SpoIIIE and 2 nM DNA (DNA_{NS} or DNA_{SRS}) were pre-incubated during 10 min at 27 °C and rapidly mixed with a 10,000 nM solution of unlabelled DNA_{NS}. More details are provided in supplementary information online. ATPase measurements were performed in reaction buffer with identical temperature conditions to those employed for FA measurements with the addition of 3 mM ATP and reagents from EnzChek Pyrophosphate Assay Kit (Molecular Probes). Protein concentration was in all cases 5 nM. More details are provided in supplementary Fig S5 online and in supplementary information online.

Fluorescence correlation spectroscopy. FCS experiments were carried out on a home-built confocal fluorescence microscope set-up. Measurements were performed in reaction buffer in absence or presence of unlabelled DNA_{SRS} (50 nM). We estimated a labelling efficiency of ~30% for monomeric SpoIIIE, thus we assume that hexamers of SpoIIIE contain between 1 or 2 fluorophores each. More details are given in supplementary information online.

AFM imaging. AFM images were obtained with a Nanoscope IIIa microscope (Veeco, France) equipped with a type-E scanner and operating in tapping mode in air using AC160 TS Olympus cantilevers. More details are given in supplementary information online.

Data analysis and modelling. Equilibrium and kinetic binding data were empirically fit with a single-site-binding model and exponential functions to obtain apparent affinities, association and dissociation rates. FCS data were fitted to an analytical 2D diffusion model containing one or two independent diffusing species (free dye and fluorescently labelled SpoIIIE). Theoretical diffusion coefficients were modelled from structural homology models of SpoIIIE on the basis of the hexameric PaFtsK structure (PDB 2IUU) or monomeric PaFtsK (PDB 2IUT) [11] using HYDROPRO [10]. Equilibrium constants for the monomer–hexamer association were obtained using BIOEQS [18]. At least three independent

preparations of purified SpoIIIE were evaluated for each experiment. Parameters were expressed as the mean ± s.e. Details on Monte Carlo stochastic modelling and fitting procedures are provided as supplementary information online.

Supplementary information is available at EMBO *reports* online (http://www.emboreports.org).

ACKNOWLEDGEMENTS

We acknowledge support for this research to the Human Frontiers Science Program (M.N. and D.I.C.) and the Institut National de la Santé et de la Recherche Médicale (M.N.). We are grateful to N. Marcotte and D. Lerner for their valuable help in kinetic measurements.

Author contributions: D.I.C. and M.N. conceived and designed the experiments; D.I.C., C.G. S.T., E.M. and P.-E.M. performed the experiments; O.C. and D.I.C. conceived software, O.C. developed software; M.N. and D.I.C. analysed the data; D.I.C. and M.N. wrote the paper.

CONFLICT OF INTEREST

The authors declare that they have no conflict of interest.

REFERENCES

1. Pease PJ, Levy O, Cost GJ, Gore J, Ptacin JL, Sherratt D, Bustamante C, Cozzarelli NR (2005) Sequence-directed DNA translocation by purified FtsK. *Science* **307:** 586–590
2. Ptacin JL, Nollmann M, Becker EC, Cozzarelli NR, Pogliano K, Bustamante C (2008) Sequence-directed DNA export guides chromosome translocation during sporulation in *Bacillus subtilis*. *Nat Struct Mol Biol* **15:** 485–493
3. Vogelmann J, Ammelburg M, Finger C, Guezguez J, Linke D, Flotenmeyer M, Stierhof YD, Wohlleben W, Muth G (2011) Conjugal plasmid transfer in Streptomyces resembles bacterial chromosome segregation by FtsK/SpoIIIE. *EMBO J* **30:** 2246–2254
4. Levy O, Ptacin JL, Pease PJ, Gore J, Eisen MB, Bustamante C, Cozzarelli NR (2005) Identification of oligonucleotide sequences that direct the movement of the *Escherichia coli* FtsK translocase. *Proc Natl Acad Sci USA* **102:** 17618–17623
5. Bigot S *et al* (2005) KOPS: DNA motifs that control *E. coli* chromosome segregation by orienting the FtsK translocase. *EMBO J* **24:** 3770–3780
6. Lowe J, Ellonen A, Allen MD, Atkinson C, Sherratt DJ, Grainge I (2008) Molecular mechanism of sequence-directed DNA loading and translocation by FtsK. *Mol Cell* **31:** 498–509
7. Bigot S, Saleh OA, Cornet F, Allemand JF, Barre FX (2006) Oriented loading of FtsK on KOPS. *Nat Struct Mol Biol* **13:** 1026–1028
8. Graham JE, Sherratt DJ, Szczelkun MD (2010) Sequence-specific assembly of FtsK hexamers establishes directional translocation on DNA. *Proc Natl Acad Sci USA* **107:** 20263–20268
9. Lakowicz JR (2006) *Principles of Fluorescence Spectroscopy*. New York: Springer
10. Ortega A, Amoros D, Garcia de la Torre J (2011) Prediction of hydrodynamic and other solution properties of rigid proteins from atomic- and residue-level models. *Biophys J* **101:** 892–898
11. Massey TH, Mercogliano CP, Yates J, Sherratt DJ, Lowe J (2006) Double-stranded DNA translocation: structure and mechanism of hexameric FtsK. *Mol Cell* **23:** 457–469
12. Halford SE, Marko JF (2004) How do site-specific DNA-binding proteins find their targets? *Nucleic Acids Res* **32:** 3040–3052
13. Burton BM, Marquis KA, Sullivan NL, Rapoport TA, Rudner DZ (2007) The ATPase SpoIIIE transports DNA across fused septal membranes during sporulation in *Bacillus subtilis*. *Cell* **131:** 1301–1312
14. Skordalakes E, Berger JM (2006) Structural insights into RNA-dependent ring closure and ATPase activation by the Rho termination factor. *Cell* **127:** 553–564
15. Lee JY, Finkelstein IJ, Crozat E, Sherratt DJ, Greene EC (2012) Single-molecule imaging of DNA curtains reveals mechanisms of KOPS sequence targeting by the DNA translocase FtsK. *Proc Natl Acad Sci USA* **109:** 6531–6536
16. Wagner T, Bellinzoni M, Wehenkel A, O'Hare HM, Alzari PM (2011) Functional plasticity and allosteric regulation of α-ketoglutarate decarboxylase in central mycobacterial metabolism. *Chem Biol* **18:** 1011–1020
17. Mott ML, Berger JM (2007) DNA replication initiation: mechanisms and regulation in bacteria. *Nat Rev Microbiol* **5:** 343–354
18. Royer CA, Smith WR, Beechem JM (1990) Analysis of binding in macromolecular complexes: a generalized numerical approach. *Anal Biochem* **191:** 287–294